Linear Geometry Hall Thruster with Boron Nitride and Diamond Walls[*†]

Nathan B. Meezan, Nicolas Gascon, and Mark A. Cappelli
Thermosciences Division, Mechanical Engineering Department
Stanford University
Stanford, CA 94305-3032
650-723-1745
cap@stanford.edu

IEPC-01-39

A preliminary assessment of the sputter resistance of polycrystalline diamond plates against xenon ion bombardment is reported, and first studies of integrating diamond walls into a Hall discharge channel are performed. The polycrystalline diamond is found to have a 25% better resistance to sputtering than boron nitride, a more commonly used Hall thruster wall material. The diamond plates were integrated into a linear Hall thruster with an open electron drift. In comparison to a similar Hall thruster with boron nitride walls, the diamond containing discharge had an overall lower discharge current, but resulted in a slightly lower propellant utilization. However, unlike the case with boron nitride walls, operation with the diamond walls was limited to 200V or higher, due to the emergence of large-scale fluctuations at lower voltages.

Introduction

Hall discharges, also called Hall thrusters or closed-drift thrusters, are presently used in satellite propulsion applications. In a typical Hall thruster, a low-pressure discharge is sustained within an annular channel, with surrounding solenoids generating a radial magnetic field. Electrons drifting towards the anode at the back of the channel are magnetized. Constrained to move in a closed, azimuthal $\boldsymbol{E} \times \boldsymbol{B}$ drift, the electrons provide an uninterrupted Hall current—hence the name "closed-drift thruster." The resultant axial electric field (a consequence of the impeded axial electron flow) accelerates the non-magnetized propellant ions (usually xenon) out of the channel. Coaxial Hall thrusters operating near 1 kW can eject ions at 15-20 km/s, producing 40-80 mN of thrust at efficiencies in excess of 50%.

Despite the impressive performance of coaxial Hall thrusters, a need has developed for low thrust, high efficiency propulsion for precise control of small satellites. While a low power Hall thruster could fill this need, scaling a coaxial thruster down in size is not trivial. In particular, a consequence of the scaling relations for Hall discharges results in significant increases in the particle and energy flux to the ceramic (electrically insulating) walls of the discharge [1,2]. It is speculated that the walls play an important role in the cross-field resistivity of the discharge. Understanding these wall effects and engineering channel wall materials for improved performance is critical to the development of low power Hall thruster technologies.

In this paper, we present a continued study of the behavior of a low-power linear-geometry Hall thruster that has an *open electron drift* [2-5], with particular attention paid to operation of the thruster with diamond walls. The linear, open-drift design was the outcome of (i) a desire to reduce $\boldsymbol{B}$-field divergence, (ii) the need to simplify manufacturability for very small scales, (iii) the desire to incorporate advanced

[*] Presented as Paper IEPC-01-39 at the 27th International Electric Propulsion Conference, Pasadena, CA, 15-19 October 2001.

ceramic materials which are not easily machined but are available in plate form, such as polycrystalline diamond, and (iv) the reasoning that electrons do not reside in the channel long enough to complete a closed $\boldsymbol{E} \times \boldsymbol{B}$ drift due to the anomalously low electron Hall parameter [6]. That electrons may not necessarily close their azimuthal drift in modern day Hall thrusters is supported by the recent Monte Carlo simulations of Degond et al. [7]. Although our past versions of our linear Hall thruster with alumina and boron nitride walls were not optimized for their magnetic field distribution and channel length, recent measurements of the thrust, thrust efficiency, and specific impulse at very low powers (~75W) were quite promising (T = 2.1 mN, η = 14.6%, I_{sp} = 1070 sec) [5].

Here, we present the results of a study on an improved thruster design operating with both boron nitride and chemically vapor deposited polycrystalline diamond walls. Based on available data in the literature, diamond is expected to have a high sputter resistance to bombarding xenon ions. Furthermore, diamond has the highest thermal conductivity of all insulators, and the lowest dielectric constant. A low dielectric constant suggests that it may have a very low low-energy secondary electron yield and low backscatter coefficient, both of which are desirable properties for the walls in Hall discharge channels. We present the results of an independent (and direct) sputter rate comparison against other possible wall materials (alumina, boron nitride, and silicon carbide). Furthermore, the availability of diamond plate material [8] permitted us to integrate diamond ceramic walls into our linear geometry thruster. Although a direct comparison in performance to that containing boron nitride walls cannot be made (due to a slight variance in thruster geometry), the Hall thruster with the diamond walls operated with a lower overall discharge current, but slightly lower propellant utilization.

Sputter Data

Any material used as a channel wall for a Hall thruster must have a high sputter resistance to xenon ion bombardment, since propulsion system life (which is often compromised by ion-induced erosion of critical components) is one of the most important factors considered in selecting a thruster for a particular mission. Fortunately, in considering various wall material options, such as alumina (Al_2O_3), boron nitride (BN), and diamond, some (albeit limited) experimental data is available on the xenon-ion induced sputter yield, that suggests that chemically vapor deposited (CVD) diamond has some sputter resistance benefits. Recently, Blandino et al. used a profilometry-based technique to quantify the sputter-yield of CVD diamond and other potential grid materials for ion engines under xenon ion bombardment [9,10]. His data is compared directly to available erosion rate data (mostly from the early Russian literature [11]) of various common wall materials for Hall thrusters in Fig. 1. In the figure, the sputter yield is given as the "volume sputtering coefficient" (the volume of material sputtered per coulomb of incident ion) and the solid line shown is a linear fit to the Blandino's four discrete data points for CVD diamond (note that the two points for diamond outside the energy range of the Russian data are not shown). The sputter yield (sputtered atoms/incident ion), which is what is tabulated for CVD diamond in Ref. 10, is converted to the volume sputtering coefficient using the known atomic weight of carbon, and the ideal mass density of diamond. Although the data is limited in extent, we see that the erosion rate for diamond is significantly less than that of boron nitride and appears to be lower than that of alumina above incident ion energies of about 150 eV. These encouraging results prompted us to perform our more direct sputter test, in the plume of a laboratory Hall thruster, as discussed in the following paragraph.

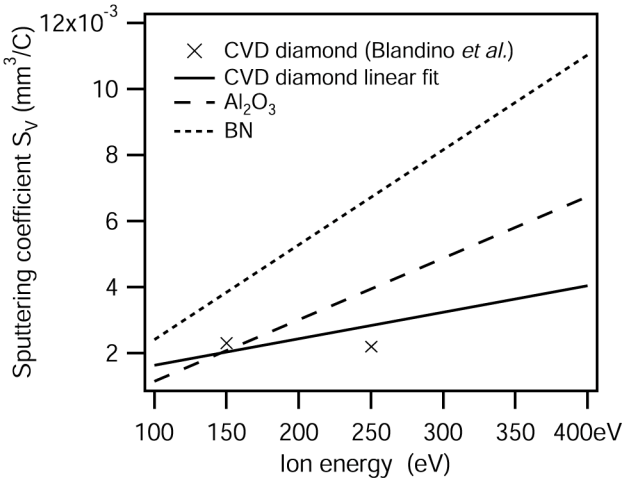

Figure 1- Sputtering coefficients for insulator materials of interest [10, 11].

In order to confirm the relative sputter resistance suggested by the data presented in Fig. 1 above, we carried out a straightforward experiment that provides a direct measure of the relative sputter yield at normal incident ion bombardment and at ion energies characteristic of Hall thrusters. Plate samples of four different ceramic materials (alumina, boron nitride, silicon carbide, and CVD diamond) were placed in the very near field plume of a laboratory Hall thruster for several hours. The samples were slightly irregular and approximately 2 cm x 1 cm x 1 mm in shape, and clamped to the front outer magnetic pole piece such that about half of each sample was exposed to the ion beam, spaced 90° apart around the circumference of the discharge. The thruster was operated at 100 V with a mass flow rate of 2 mg/s xenon for 10 hours. Under these conditions, we estimate the ion energy at the thruster exit to be around 50 eV, accounting for cathode and anode fall losses, and past experimental results that indicate that a significant fraction of the ion acceleration takes place beyond the axial location of the outer pole piece. Due to the azimuthal symmetry of the Hall thruster, each sample was exposed to approximately the same ion beam conditions.

The samples were weighed before and after exposure to the ion beam. Using the mass density of each sample, determined by Archimedes' method, we translated the mass change into a sputtered volume. The sputtered volume was then divided by the exposed area of the each sample to give an average erosion depth.

The erosion depth of each sample is given in Table 1. The results seen from this relatively straightforward exercise are remarkably consistent with the data presented in Fig. 1. Alumina is found to have the lowest erosion rate (for these 50 eV ions), followed by CVD diamond, silicon carbide, and boron nitride. The results provide the impetus for trying CVD diamond as a potentially beneficial wall material in a working Hall thruster, since it will erode at a rate that is no worse than BN, a common Hall thruster wall material. However, since mm-thick CVD diamond is not available in cylindrical shapes suitable for integration into a co-axial discharge geometry, we instead performed these studies in our lower-power linear-geometry Hall thruster. The performance of this thruster operating with either boron nitride or CVD diamond walls is measured through the characterization of the distributed and total ion beam current and propellant utilization, recorded by a translating ion probe in the near field of the thruster plume.

Table 1. Erosion Depth of Various Insulator Materials after 10 hours of Exposure to Hall Thruster Plume.

Sample material	Erosion depth (μm)
Al_2O_3	3.56
Diamond	7.87
SiC	8.97
BN	11.13

Ion Current Experiments

Thruster

The design and performance of the first linear Hall thruster are described in detail in previous papers [3-5]. We have recently developed a second discharge, incorporating design improvements to allow stable operation at high voltage. The discharge and the experimental set-up, along with the coordinate system used in this paper, are shown in Fig. 2. The magnetic circuit was built from cast gray iron and consisted of two rectangular solenoid coils, two front pole pieces, and one back pole piece. A magnetic screen was also used to sharpen the magnetic field profile. The circuit is capable of a peak magnetic field strength of 1500 gauss at 3 A of coil current; however, the coil current was kept below 1 A under vacuum to prevent melting of the kapton wire insulation. The magnetic field profile in the axial (z) direction for the nominal

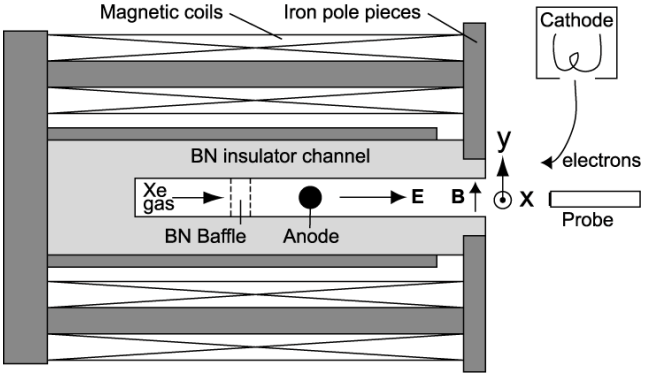

Figure 2 - Linear Hall thruster design details (BN channel)

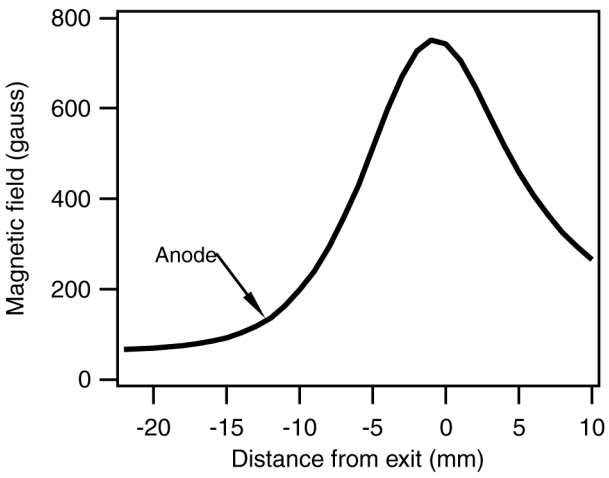

Figure 3-Magnetic field profile for the linear Hall thruster

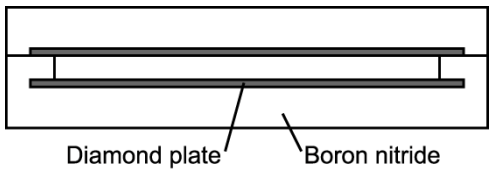

Figure 4-Schematic of diamond channel design

operating coil current of 1 A is shown in Fig. 3. The peak field for this condition is approximately 800 gauss, and the field strength at the anode is over 100 gauss. The field had excellent uniformity (< 1 % variation) along the *x* direction.

Two different discharge channels were constructed to allow testing of different wall materials. The first channel is a boron nitride box approximately 50.8 mm in *x*, 3.2 mm in *y*, and 12.7 mm from anode to exit. The second channel, also made of boron nitride, was machined with two pockets that allow rectangular plates of different wall materials to be clamped into place, as shown in Fig. 4. For the diamond thruster, we used 1 mm thick plates of pure CVD diamond provided by SP^3 Inc. [8]. The surfaces facing the plasma were polished to a mirror finish. In both channels, a boron-nitride baffle separates a plenum from the anode, a tungsten rod 1.6 mm in diameter. A commercial hollow cathode discharge neutralizer (Veeco/IonTech HCN-252) was used to neutralize the ion beam. The cathode was located 28 mm downstream of the channel exit, 45 mm from the channel in *y* and centered in *x*. The thruster was generally operated with 0.6 mg/s of xenon through the anode and 0.3 mg/s of xenon through the cathode. Both the BN-channel and diamond-channel thrusters proved capable of continuous operation at voltages as high as 300 V.

The length of the channel in *x* relative to the characteristic axial scale length defined by the zone of ionization (~5 mm in many modern Hall thrusters) was chosen such that:

$$\frac{L_x}{L_{i_z}} \approx \frac{J_{ex}}{J_{ey}} >> 1 \qquad (1)$$

This condition is imposed on the design, so that electrons have sufficient opportunity to cross the imposed magnetic field (as a result of either fluctuations in the electric field, or wall scattering). It is found in a typical Hall discharge against which this linear discharge was scaled [3], that within the ionization zone, the ratio:

$$\frac{J_{ex}}{J_{ey}} = \left(\omega_{ce}\tau_e\right)_{eff} \sim O\left(10-100\right) \qquad (2)$$

Here, $\left(\omega_{ce}\tau_e\right)_{eff}$ is the electron Hall parameter, which characterizes the extent to which the electrons are magnetized. In this most recent linear discharge design, the aspect ratio of the channel given by Eqn. 1 above is at the low end of the condition imposed by Eqn. 2, suggesting that some end effects are likely to be encountered with the thruster reported on here.

Vacuum Chamber

All experiments were performed in a stainless steel vacuum chamber pumped by two 20-inch diffusion pumps (without baffles). This pumping plant provided an operating pressure of 7×10^{-5} torr at the nominal operating condition, as measured by an ionization gauge uncorrected for xenon. Separate DC power supplies powered the anode, cathode heater, cathode keeper, and magnet coils. The cathode body was kept at tank (ground) potential. The discharge voltage and current were monitored with digital multimeters. Discharge current oscillations were measured with a powered differential amplifier (Tektronix P5200)

placed across a 4 Ω series resistor and recorded by a high-speed PC-based digital oscilloscope (National Instruments PCI-5102).

Ion Probe

To profile the ion-current density, we scanned a planar probe over a 80 mm by 36 mm rectangle with a grid-spacing of 5 mm in *x* and 3 mm in *y*, at downstream distances of 15 mm and 30 mm. The probe, a 1.6 mm diameter tungsten rod shielded by an alumina (Al_2O_3) sleeve, was biased at –20 V to insure all electrons were repelled (no corrections were made for the possible contributions of secondary electron current). The probe current was split between two 100 W resistors. A high-common mode differential amplifier (Burr Brown/Texas Instruments INA117) was used to measure the time-dependent ion current, while a GPIB-capable digital multimeter (Fluke 8840A) measured the mean ion-current. The probe current and discharge current were recorded simultaneously at each point in the scan.

Results

Oscillations

A discharge current-voltage curve for the BN thruster is shown in Fig. 5. The figure displays both the mean current, and the amplitude of the oscillations. It is seen that this linear Hall discharge displays only a slight region of saturation (and possibly a region of negative resistance), for discharge voltages less than 150V, followed by a gradual increase in discharge current at voltages ranging from 150 – 300 V. The region below 150 V is concomitant with the appearance of the "breathing" mode (discussed below) – a behavior characteristic of co-axial Hall discharges [12], characterized by strong amplitude oscillations. The gradual rise in the current beyond 150V is

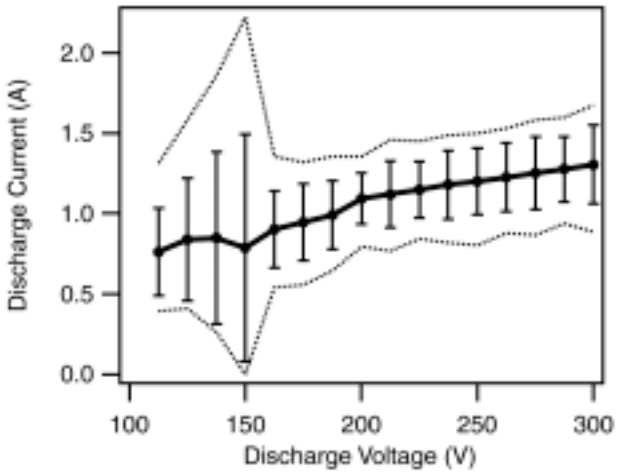

Figure 5-Current-voltage characteristic and oscillation amplitudes of linear Hall thruster with BN walls. Error bars indicate the standard deviation of the oscillating current. Dotted lines are plotted at the top tenth and bottom tenth of the current oscillation range.

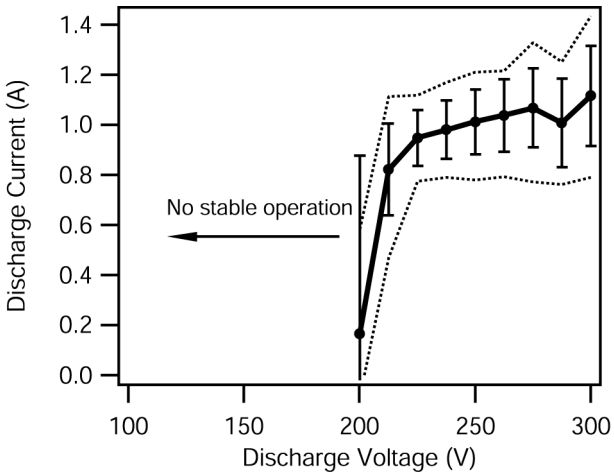

Figure 6- Current-voltage characteristic and oscillation amplitudes of linear Hall thruster with diamond walls. Error bars and dotted lines are as in Fig. 5.

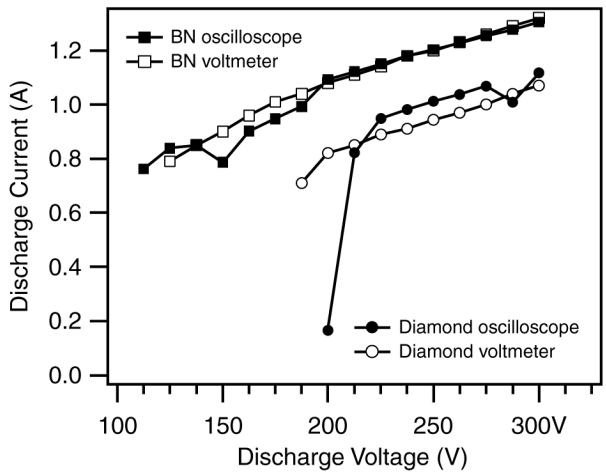

Figure 7 - Comparison of mean current-voltage characteristics for diamond and BN walls, measured with both a digital oscilloscope (black symbols) and a digital voltmeter (open symbols).

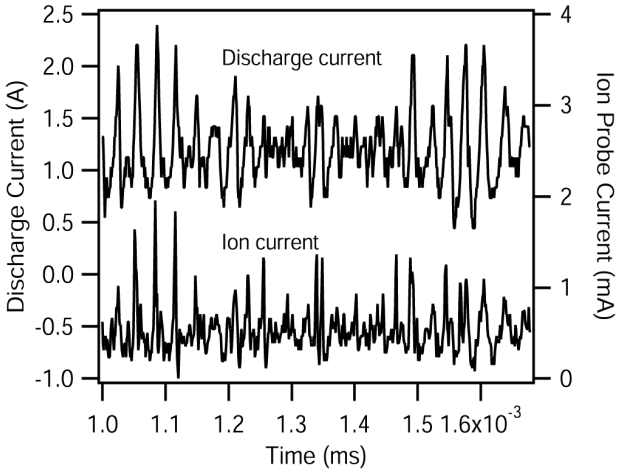

Figure 8 - Sample waveforms recorded for the BN thruster with probe located at the center of the channel ($x = 0$, $y = 0$).

unusual, and suggestive of an enhanced electron current, quite possibly due to the end wall effects, with a high flux of drifting electrons striking the end walls and adding to the near-wall conductivity.

The discharge current - voltage characteristic for the case of the diamond walls is shown in Fig. 6. This I-V characteristic is very different than that of the thruster with the boron-nitride wall. The addition of the diamond walls precluded operation below 200V, as the discharge became exceptionally unstable. Also, at the highest voltages studied, the diamond walls permitted operation at much lower total discharge current, as seen from the mean current monitored with a digital voltmeter (see Fig. 7).

Typical raw data for the ion and discharge currents are shown in Fig. 8, for the case of BN walls and 250V operation. The expected "breathing" oscillation at 35 kHz is evident, along with a lower-frequency envelope of unknown origin. The two traces are in phase and are virtually identical in shape. Assuming the discharge-current is nearly constant over the course of a scan, we can use it as the time-base for temporal reconstruction of the local ion-current density. We do this using an integrating histogram. We divided the (total) discharge current into five amplitude ranges and further divided the middle ranges into "rising" or "falling," resulting in eight bins. At each point in time, the ion current is added to one of the bins, based on the value and slope of the discharge current. This procedure is repeated at each point in x-y space to reconstruct the entire ion current.

The resulting images (Fig. 9) reveal a bulk oscillation typical of Hall thrusters operating in the "breathing" mode. This behavior in coaxial thrusters has been captured in high-speed optical experiments and in numerical models [13,14]. The origin of this instability is simply particle conservation [15]. The ionization and subsequent acceleration of gas particles in the ionization zone locally depletes the neutral density. The ionization rate, ion density, and ion current decrease until slow-moving neutrals can replenish the channel, producing a "predator-prey" type instability [16]. Although not shown here in this paper, the results for the case of the diamond wall are qualitatively similar to those shown in Fig. 9.

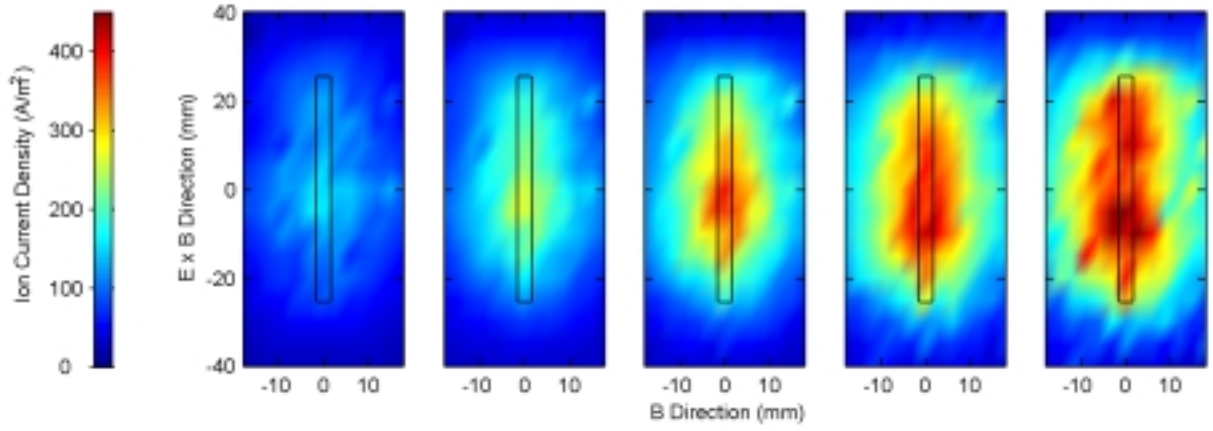

Figure 9 - Breathing oscillation "movie" for BN thruster at 200 V operation.

The oscillation frequency of this breathing mode should rise monotonically with voltage, as the mean ion velocity increases. This is observed in the top rendering of Fig. 10, for the BN case. The spectra shown in Fig. 10 are taken at intervals of 12.5 V. There are two distinct operating regimes regions apparent from the data for the boron nitride channel. Between 125 and 175 V, the peak oscillation amplitude increases rapidly, showing distinct oscillation frequencies and associated harmonics. Beyond 175 V, the oscillation amplitude decreases, while the bandwidth increases. While a direct comparison to the case of the diamond channel (lower frame in Fig. 10) is difficult to make, since the thruster would not operate below 200V, it is apparent that at the lowest voltages, the diamond channel was highly unstable to the point of extinction. With increasing voltage, the amplitude of the oscillations diminished, followed subsequently with the appearance of very strong disturbances at 300V.

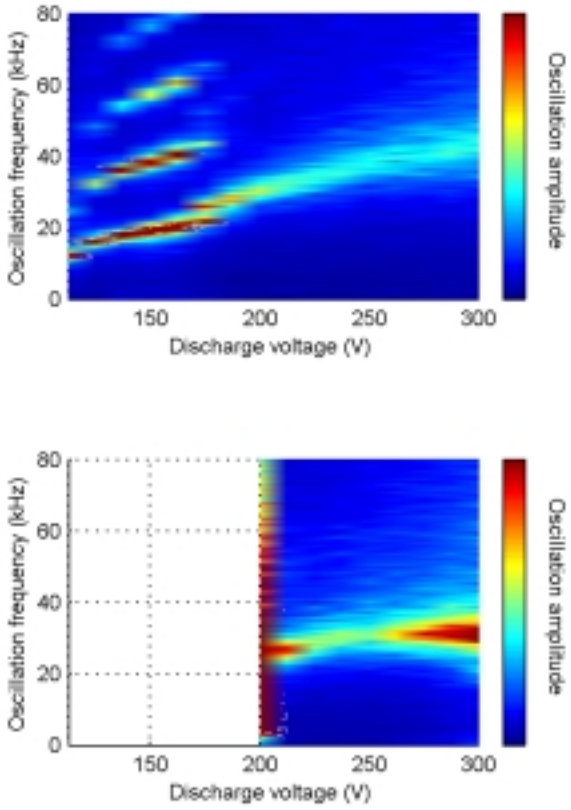

Figure 10 - Current oscillation spectra for the case of a BN channel (top) and for the diamond channel thruster (bottom).

Performance

Integrating the time-average ion current density over the scan area gives a mean ion-current of 0.45 A for the BN thruster operating at 250 V. This corresponds to a propellant utilization of 105 %, where the propellant utilization is defined as the ratio of the total ion-current to the "mass-flow current," i.e., the current given by 0.6 mg/s of singly-ionized xenon. The fact that the measured ion current is greater than the mass-flow current could indicate the presence of doubly ionized xenon; however, it is more likely due to error in the ion current measurement. The ion current can be over-predicted due to expansion of the probe sheath at the –20 V bias and due to ion-induced secondary electron generation at the probe surface. Within experimental uncertainty, we can only say that the propellant utilization is quite high. However, the ratio of ion current to total current is 0.38. So, while the specific impulse of the linear thruster studied here may be comparable to that of a large coaxial Hall thruster, its thrust efficiency will be considerably lower.

Remarkably, the overall spatial distribution of the time-averaged ion current downstream of the thruster is generally the same for the two wall material cases (see Figs. 11, 12). Within 15 mm and 30 mm from the exit plane, the ion plume has expanded with an estimated divergence of 15^{o} in the transverse (parallel to $\boldsymbol{B}$) direction, and 60^{o} in the lateral (parallel to the $\boldsymbol{E} \times \boldsymbol{B}$) directions. The higher divergence along the lateral direction is expected, based purely on geometric arguments, and is a feature that is somewhat unique to these linear geometries. This strong lateral divergence may be problematic to those concerned about plume impact on nearby satellite components such as solar panels.

At the same operating voltage and mass flow (250 V, 0.6 mg/s), the mean ion current for the diamond walled thruster was 0.34 A, giving a propellant utilization of only 78 %. While this value is lower than the BN thruster, the total current of the diamond thruster is also much lower: the diamond thruster's ratio of ion current to total current of 0.33 is very close to that of the BN thruster, predicting a similar thrust efficiency. Previous studies of Hall thruster wall materials [17] have shown that changing the wall

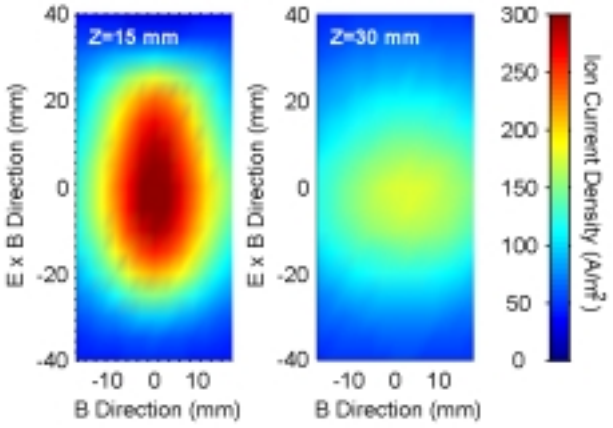

Figure 11 - Mean ion current profiles for BN thruster.

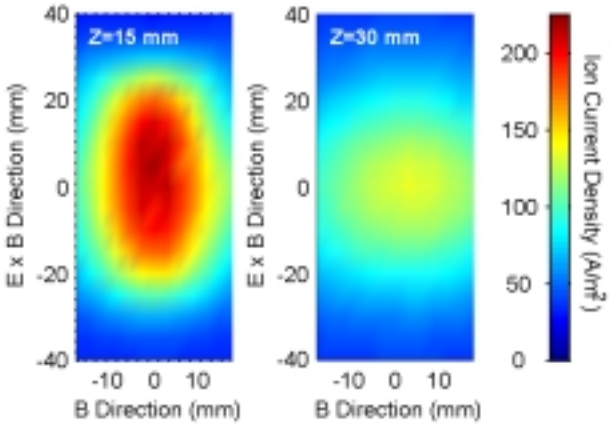

Figure 12 - Mean ion current profiles for diamond thruster.

material tends to change the total discharge current and discharge power with little impact on the ion behavior, i.e., the thrust. We expected this kind of behavior in the linear thruster and were surprised to see both a lower discharge current and ion current for the diamond channel.

There are several possible causes for this behavior. The rate of electron-wall collisions and their importance to electron transport and energy transport in a Hall thruster depends on the secondary electron emission coefficient of the wall material. The surface roughness, electrical conductivity, and stopping power (the rate at which an electron traveling into the lattice loses energy) can also be important in determining the effects of a dielectric wall on the plasma behavior, in particular, the so-called "near-wall" electron conductivity.

Changing the electron conductivity in the thruster will alter the electron temperature of the plasma, changing the ionization rate. The location of the ionization zone in the channel may also move, changing the divergence of the ion beam. Unfortunately, we must explore areas of experimental uncertainty before we can speculate on the physical mechanisms behind the diamond thruster's performance. It is noted that the gas propellant systems in the two thruster channels were very similar, but not identical. The gas baffle in the diamond thruster was thicker and closer to the anode than in the BN channel. In hindsight, we think these minor differences in design may be significant, and can account for much of the differences in the I-V curves seen, and in the discharge stability. Future tests are planned for operating the second channel with 1 mm thick BN inserts, so that the two wall materials can be compared under exactly the same channel configurations.

Summary

These experiments on the relative sputter yield of diamond verses other potential Hall discharge wall materials provide an impetus for further studies on possible performance benefits associated with the integration of diamond technology into modern Hall thrusters. The sputter resistance of diamond under conditions of ion bombardment expected at the exit of a Hall thruster has been found to be a factor of about 25% better than that of boron nitride, a result consistent with prior available data in the published literature. When integrated into a low-power linear geometry source, we found that the diamond resulted in a relatively low total discharge current in comparison to the case of a pure boron nitride channel, although slight differences in the injector geometry precluded a direct comparison. In both cases, i.e., that of boron-nitride walls and diamond walls, the linear Hall thruster resulted in an ion beam profile that was highly asymmetric, with an anisotropic beam divergence of 15^{o} (in the direction of **B**) and 60^{o} (parallel to the **E** x **B** direction). Unlike the case with boron nitride walls, operation with the diamond walls was limited to 200V or higher, due to the emergence of large-scale fluctuations at lower voltages.

Acknowledgements

The authors would like to thank J. Zimmer and J. Herlinger, at sp^3 Inc., for providing the diamond samples, F. Levy for help with the fabrication of the channel, and P. Degond and S. Barral for stimulating discussions. This research was supported by the Air Force Office of Scientific Research. A fellowship for N.Gascon was provided by the European Space Agency. Support for N. Meezan is supported by the Stanford Graduate Fellowship program.

References

[1] V. Khayms and M. Martinez-Sanchez, "Design of a Miniaturized Hall Thruster for Microsatellites," AIAA -96-3291, 32nd Joint Propulsion Conference, Lake Buena Vista, FL, July 1-3, 1996.

[2] D. P. Schmidt, N.B. Meezan, W.A. Hargus, Jr., and M.A. Cappelli, "A Low-Power, Linear-Geometry Hall Plasma Source with an Open Electron-Drift," *Plasma Sources Science and Technology* **9**, 68-76, 2000.

[3] W.A. Hargus and M.A. Cappelli, "Development of a Linear Hall Thruster," AIAA-98-3336, 34th Joint Propulsion Conference, Cleveland, OH, July, 1998.

[4] M.A. Cappelli, D. Schmidt, N. B. Meezan, and W.A. Hargus Jr., "Continued Development of a Linear Hall Thruster," AIAA-99-2569, 35th Joint Propulsion Conference, Los Angeles, CA, June 20-24, 1999.

[5] M.A. Cappelli, Q.E. Walker, N.B. Meezan, W.A. and Hargus, Jr., "Performance of a Linear Hall Discharge with an Open Electron Drift" AIAA-2001-3503, 37th Joint Propulsion Conference, Salt Lake City, UT, July 8-11, 2001.

[6] N.B. Meezan, W. A. Hargus, Jr., and M. A. Cappelli, "Anomalous Electron Mobility in a Coaxial Hall Discharge Plasma", *Physical Review E* **63**, 026410, 2001.

[7] V. Latocha, L. Garrigues, P. Degond, and J.P. Boeuf, "Numerical Simulation of Electron Transport in Stationary Plasma Thrusters," *in press*, 2001.

[8] The diamond was provided by sp^3 Inc., 505 East Evelyn Ave., Mountain View, CA.

[9] J. J. Blandino, D. G. Goodwin, and C. E. Garner, "Low Energy Sputter Yields for Diamond, Carbon-Carbon Composite, and Molybdenum Subject to Xenon Ion Bombardment," *Diamond and Related Materials* **9**,1992-2001, 2000.

[10] J. J. Blandino, "Application of Diamond Films to Electric Propulsion: Low Energy Sputter Yield Measurement and MPD Plasma Assisted Chemical Vapor Deposition," Ph.D. Thesis, California Institute of Technology, Pasadena, CA, 2001.

[11] V. V. Egorov et al. in Ion Injectors and Plasma Thrusters [in Russian, eds. A. I. Morozov and N. N. Semashko] (Moscow: Energoatomizdat, 1990), 56-61, figure rpt. in A. I. Morozov and V. V. Savelyev, "Fundamentals of Stationary Plasma Thruster Theory," Review of Plasma Physics vol. 21 eds. B. B. Kadomtsev and V. D. Shafranov (New York: Consultants Bureau) 244.

[12] N. Gascon, C. Perot, G. Bonhomme, X. Caron, S. Bechu, P. Lasgorceix, B. Izrar, and M. Dudek, "Signal Processing and Non-Linear Behavior of a Stationary Plasma Thruster: First Results," AIAA-99-2427, 35th Joint Propulsion Conference, Los Angeles, CA, June 20-24, 1999.

[13] F. Darnon, M. Lyszyk, and A. Bouchoule, "Optical Investigation on Plasma Oscillations of SPT Thrusters, AIAA-97-3051, 33rd Joint Propulsion Conference, Seattle, WA, July 6-9, 1997.

[14] J.P. Boeuf and L. Garrigues, "Low Frequency Oscillations in a Stationary Plasma Thruster, *J. Appl. Phys*. **84**, 3541-3554, 1998.

[15] E.Y. Choueiri, "Plasma Oscillations in Hall Thrusters," *Physics of Plasmas* **8**, 1411-1426, 2001.

[16] J. Fife and M. Martinez-Sanchez, "Comparison of Results from a Two-Dimensional Numerical SPT Model with Experiment." AIAA -96-3197, 32nd Joint Propulsion Conference, Lake Buena Vista, FL, July 1-3, 1996.

[17] Y. Raitses, J. Ashkenazy, G. Appelbaum, and M. Guelman, "Experimental Investigation of the Effect of Channel Material on Hall Thruster Characteristics," 25th International Electric Propulsion Conference, Cleveland, OH, August 24-28, 1997.